

## **General Disclaimer**

### **One or more of the Following Statements may affect this Document**

- This document has been reproduced from the best copy furnished by the organizational source. It is being released in the interest of making available as much information as possible.
- This document may contain data, which exceeds the sheet parameters. It was furnished in this condition by the organizational source and is the best copy available.
- This document may contain tone-on-tone or color graphs, charts and/or pictures, which have been reproduced in black and white.
- This document is paginated as submitted by the original source.
- Portions of this document are not fully legible due to the historical nature of some of the material. However, it is the best reproduction available from the original submission.

**NASA TECHNICAL  
MEMORANDUM**

**NASA TM-78828**

(NASA-TM-78828) STRAINRANGE PARTITIONING  
BEHAVIOR OF THE NICKEL-BASE SUPERALLOYS,  
RENE' 80 AND IN 100 (NASA) 17 p HC A02/MF  
A01 CSCL 11F

N78-21267

Unclas  
12432

G3/26

NASA TM-78828

**STRAINRANGE PARTITIONING BEHAVIOR OF THE  
NICKEL-BASE SUPERALLOYS, RENÉ 80 AND IN 100**

by G. R. Halford and A. J. Nachtigall  
Lewis Research Center  
Cleveland, Ohio 44135

TECHNICAL PAPER to be presented at the  
Forty-sixth Meeting of the Structures and Materials  
Panel of AGARD Specialists' Meeting on Characterization  
of Low Cycle High Temperature Fatigue by Strainrange  
Partitioning Method  
Aalborg, Denmark, April 9-14, 1978



## STRAINRANGE PARTITIONING BEHAVIOR OF THE NICKEL-BASE SUPERALLOYS, RENE' 80 AND IN 100

G. R. Halford and A. J. Nachtigall, Engineers  
National Aeronautics & Space Administration  
Lewis Research Center  
21000 Brookpark Road  
Cleveland, OH 44135  
USA

ORIGINAL PAGE IS  
OF POOR QUALITY

## ABSTRACT

A study has been made to assess the ability of the method of Strainrange Partitioning (SRP) to both correlate and predict high-temperature, low-cycle fatigue lives of nickel-base superalloys for gas turbine applications. Baseline data from strain-controlled, low-cycle fatigue tests are expressed in terms of the PP, PC, CP, and CC partitioned inelastic strainrange versus life relationships for coated and uncoated Rene' 80 at 1000°C, Gatorized (creep-formed) IN 100 at 760°C, and cast IN 100 at 925°C. SRP is shown to correlate the cyclic lives of the baseline tests to within factors of nearly two.

The partitioned strainrange versus life relationships for uncoated Rene' 80 and cast IN 100 have also been determined from the Ductility Normalized-Strainrange Partitioning (DN-SRP) equations. These were used to predict the cyclic lives of the baseline tests. Predicted and observed cyclic lives agreed to within factors of nearly three.

The life predictability of the method is also verified for cast IN 100 by applying the baseline results to the cyclic life prediction of a series of complex strain-cycling tests with multiple hold periods at constant strain. Predictions were within factors of two in cyclic life.

It is concluded that the method of SRP can correlate and predict the cyclic lives of laboratory specimens of the nickel-base superalloys evaluated in this program.

## INTRODUCTION

Strainrange Partitioning (SRP) is a method for dealing with high-temperature low-cycle fatigue failures of metallic materials. Introduced in 1971 by Manson, Halford, and Hirschberg (Ref. 1) of the NASA-Lewis Research Center, it has been undergoing continual development since then. To-date, over 50 technical papers have been written on various aspects of the method. As a result, new dimensions in understanding, refinement of procedures, extension to new applications, or simply more laboratory specimen data for a variety of important engineering alloys have been added. Professor Manson, in his introductory paper (Ref. 2) to this Specialists Meeting, reviews the highlights of many of these past achievements and points to worthy areas for future exploration.

Although considerable experience has been gained with the use of the method of SRP at the laboratory level over the past 7 years, it seems likely that more will be required before the method can be used with confidence in the design of aeronautical gas turbine hardware and other high-temperature, high performance equipment. This AGARD Specialists Meeting thus represents a significant milestone in the development of the method because of the large number of independent laboratories that are reporting on their experiences with its use at the laboratory level of evaluation.

Owing to the nature of this Specialists Meeting, it is assumed that the reader is familiar enough with the basic concepts and terminology associated with the method of SRP that a review is not required herein. If additional background is needed, references 1 to 5 should be consulted. However, certain words are used frequently throughout this paper which are best defined at the outset so that the reader has a better understanding of the context in which they are used.

**Baseline** - Refers to the high-temperature, low-cycle fatigue tests and results used directly in the establishment of the four SRP inelastic strainrange versus life relationships.

**Verification** - Refers to the non-baseline high-temperature, low-cycle fatigue tests and results used to check how well the established SRP life relationships can be used to predict cyclic lives.

**Correlation** - Refers to how well the equations of the established SRP life relationships represent the individual baseline data. The smaller the deviation of the baseline data from the equations, the better the correlation.

**Prediction** - Refers to how well the equations of the established SRP life relationships represent the verification test results. The smaller the deviation of the verification data from the equations, the better the predictability. Since the Ductility Normalized-Strainrange Partitioning (DN-SRP) life relationships (Ref. 6) did not use any information from the baseline tests, it is considered that predictions of the baseline results are being made when using the DN-SRP equations. These equations can also be used to predict the verification results.

The objectives of this paper were to determine how well the method of SRP can both correlate and predict the high-temperature, low-cycle fatigue lives of specimens of advanced gas turbine alloys. Two nickel-base superalloys were selected for this purpose: Rene' 80 with and without an aluminide (Codep B-1) coating, and IN 100 in the Gatorized (creep-formed) and cast conditions. The four partitioned inelastic strainrange versus life relationships (PP, PC, CP, and CC) were established for each alloy condition using a series of baseline stress-hold, strain-limited tests to introduce creep strains into the cycles. In addition, an evaluation was made of how well the life relations could be determined by the recently proposed DN-SRP equations.

A limited number of verification tests were also performed with specimens of cast IN 100 using a series of complex strain cycles involving multiple periods of constant strain hold which introduced creep through the process of relaxation. The verification tests were used to evaluate the predictability of the SRP method.

#### EXPERIMENTAL DETAILS

The high-temperature, low-cycle fatigue test results were obtained in the fatigue laboratory of the NASA-Lewis Research Center using closed-loop, servo-controlled, electro-hydraulic testing machines. Hirschberg has described this facility in detail in Ref. 7. Testing was performed in a still air environment using axially loaded specimens with diametral extensometry.

#### Specimens, Materials, and Temperatures

Two specimen geometries were employed, the tubular, hour-glass shaped specimens described in Ref. 7, and a smaller, solid hour-glass shaped specimen with a minimum test section diameter of 5 mm and a 40 mm hour-glass radius. Threaded ends were provided for gripping. Overall length was 75 mm. Two nickel-base superalloys were studied, each in two different conditions; cast Rene' 80 with and without an aluminide coating, and IN 100 in the Gatorized and cast conditions. The chemical compositions, processing and heat treatment, and mechanical properties at room temperature and the elevated temperature of interest for each alloy are presented in Tables I, II, and III respectively of Appendix 1.

**Rene' 80** - The Rene' 80 specimens were supplied by TRW, Inc. under contract to NASA (Ref. 8). Enough specimens were prepared at the time for the testing program conducted in air and reported in this paper, and for the vacuum program conducted at TRW, Inc. and reported upon at this Specialists Meeting by Kortovich and Sheinker (Ref. 9). The intent of the air and vacuum programs was to establish a data base for assessing the effects of environment and protective coatings on the high-temperature low-cycle fatigue behavior of Rene' 80. The specimens were cast as individual solid bars and were subsequently machined to the tubular hour-glass shape. Half of the specimens were left uncoated and the remainder coated with an aluminide (Codep B-1) coating. Details of the coating process can be found in Ref. 8.

The coating thickness was approximately 0.05 mm. The stress and strain calculations for the coated specimens were based upon their room temperature dimensions prior to the application of the coating, i.e., it was assumed that the coating carried none of the applied load at the test temperature of 1000°C.

**Gatorized IN 100** - IN 100 was tested in the Gatorized (creep-formed) condition. Small solid specimens of this alloy were machined from a segment of a gas turbine disk (provided by Pratt & Whitney Aircraft, Florida) that had been creepformed by the Gatorizing process.

The exact chemical composition, processing heat treatment, and mechanical properties are not known, although this batch of material would be expected to be similar to the Gatorized IN 100 material reported on at this Specialists Meeting by VanWanderham, Wallace, and Annis (Ref. 10) of Pratt & Whitney Aircraft, Florida. Tests were conducted at 760°C.

**Cast IN 100** - Tubular, hour-glass shaped specimens of IN 100 were individually cast to near final dimensions. Approximately 0.2 mm thickness of material was machined from the inside and outside diameters to produce the finished test section dimensions. No heat treatment was applied to the cast specimens. Tests were conducted at 925°C.

#### SRP Test Procedures

The high-temperature, low-cycle fatigue tests were performed using the procedures recommended by Hirschberg and Halford (Ref. 5). Schematic stress-strain hysteresis loops are shown in Figs. 1(a)-(d) for the types of cycles used in conducting the baseline tests to establish the four SRP life relationships. The strain-controlled PP type test cycles (Fig. 1(a)) were applied using either a triangular or sinusoidal strain versus time waveform at a frequency of 0.5 to 1.0 Hz. In analyzing the results of the PP type tests, it was assumed that the imposed strain rates were high enough to preclude the occurrence of creep strain, thus producing inelastic strains that could be classified as plasticity. For the PC, CP, and CC type cycles, the creep strain was imposed by controlling the load on the specimen at a constant value until the desired creep strain limit was reached, whereupon, the loading direction was reversed and the other half of the cycle was imposed. If it was desired to impose creep strain in this portion of the cycle, the load was again held at a constant value until the desired opposite creep strain limit was attained, or if plasticity was desired, the specimen was rapidly loaded until the opposite strain limit was reached. The time required for the plasticity portion of the cycle was on the order of 0.5 to 2.0 seconds.

Since one of the objectives of the program was to verify the predictive capability of SRP, a series of verification tests was performed which featured test cycles quite different from those used in the baseline tests for establishing the SRP life relations. The type of cycle selected contained periods of constant strain during which creep strain accumulated through the process of stress relaxation. Stress relaxation is, of course, a frequently encountered condition in many high-temperature thermal fatigue problems. From the point of view of interpretation by SRP, creep strain accumulated either by stress relaxation or by direct constant stress creep is equally damaging.

A schematic representation of the verification test cycle is shown in Fig. 2 for the case of the multiple tensile relaxation cycle (MTRC). A duplicate series of tests, but with a multiple compressive relaxation cycle (MCRC) was also performed. The essential advantage of this type of cycle is that a considerable amount of creep strain can be accumulated for a fixed time per cycle. For the present case, the total amount of creep strain encountered with three hold periods of nearly two minutes each was about twice that which could have been obtained with a single hold period of six minutes at the peak strain. The short hold period of a few seconds at the one extreme of the strain cycle was introduced as a matter of testing convenience only. The fact that a component of completely reversed creep strain (CC) was introduced was taken into account when partitioning the inelastic strainranges and predicting the lives of these tests.

## RESULTS AND DISCUSSION

### Baseline SRP Evaluation

A complete listing of the baseline high-temperature, low-cycle fatigue data generated in this program is given in Table IV of Appendix 1 for each of the alloy conditions investigated. Sufficient information is included to perform a thorough SRP evaluation, or if so desired, an interpretation of the results in terms of other high-temperature, low-cycle fatigue approaches such as those described in Refs. 11-17. The four SRP life relationships for each alloy condition were established following the procedures described in Ref. 5. Each life relationship was expressed in terms of a power law equation relating the inelastic strainrange and cyclic life. The coefficients and exponents were determined using a least squares curve fit technique. The resultant life relationships are presented in Figs. 3, 4, and 5 for Rene' 80, Gatorized IN 100, and cast IN 100, respectively.

Rene' 80 - cursory examination of the data for coated Rene' 80 and comparison with the uncoated results did not reveal significant differences. Hence, the PP, PC, CP, and CC life relationships were established for the combined data set. The least squares curve fit SRP life relationships for Rene' 80 at 1000°C are presented in Figs. 3(a)-(e) and are listed below:

$$\begin{array}{ll} \Delta \epsilon_{PP} = 0.062(N_{PP})^{-0.51} \\ \Delta \epsilon_{PC} = 0.116(N_{PC})^{-0.64} \\ \Delta \epsilon_{CP} = 0.034(N_{CP})^{-0.45} \\ \Delta \epsilon_{CC} = 0.051(N_{CC})^{-0.49} \end{array} \quad \begin{array}{l} \text{Rene' 80} \\ 1000^{\circ}\text{C} \\ \text{Least Squares Fit} \end{array} \quad \text{EQ(1)}$$

Because the scatter in the data is nearly a factor of two in life (see for example, the PP results in Fig. 3(a)), the least squares curve fits should not be extrapolated much beyond the current range of data. The assumption that the coated and uncoated data could be considered to be of the same population is borne out in Fig. 3(f) where it can be seen that coated and uncoated results are evenly distributed above and below the central 45 degree perfect agreement line. Life differences between coated and uncoated specimens, however, may become important when the life times become significantly greater than those involved in the current program. Techniques for anticipating potential differences will be discussed in a later section.

As seen from Fig. 3(e), the four SRP life relationships for Rene' 80 do not exhibit appreciable differences over the range of variables studied. The PC, CP, and CC lives do not differ by more than a factor of two from the PP life at any given strainrange. This feature should be considered as a virtue of the Rene' 80 alloy. The alloy, as most recent cast nickel-base superalloys, has been tailored to resist creep, principally by strengthening the grain boundaries so as to resist grain boundary sliding. Thus, not only is the alloy resistant to conventional/monotonic creep rupture, it is also resistant to creep introduced in cyclic straining tests such as those reported upon in this paper. This behavior is in sharp contrast to that exhibited by some other alloys that also see service at temperatures within their creep regime. For example, the austenitic stainless steels (which are susceptible to grain boundary sliding during creep) exhibit PP and CP lives that differ by a factor of 20 for the same inelastic strainrange (Ref. 3).

Although the inelastic strainrange versus life relationships for Rene' 80 at 1000°C do not show a strong dependency on creep, the relationship between total strainrange and cyclic life can be drastically influenced by creep. This is especially true at low strainranges. The reason for this is simple. The total strainrange consists of the sum of the elastic and inelastic strainranges. The introduction of creep strain is done at the expense of elastic strain, and hence, the greater the amount of creep, the lower the elastic strainrange and the greater the inelastic component of the total strainrange. The corresponding decrease in cyclic life which is evident in Fig. 3(e) for the PC, CP, and CC relationships thus is essentially a direct result of the greater inelastic strainrange.

Gatorized IN 100 - The least squares curve fit of the SRP data for Gatorized IN 100 at 760°C are presented in Figs. 4(a)-(e). The equations of the life relationships are given below

Gatorized IN 100760°CLeast Squares Fit

$$\begin{aligned}
 \Delta \epsilon_{PP} &= 0.276(N_{PP})^{-0.80} \\
 \Delta \epsilon_{PC} &= 0.140(N_{PC})^{-0.87} \\
 \Delta \epsilon_{CP} &= 0.029(N_{CP})^{-0.43} \\
 \Delta \epsilon_{CC} &= 0.084(N_{CC})^{-0.62}
 \end{aligned}
 \quad \text{EQ(2)}$$

Because of the limited quantity of available material, few tests could be conducted with this alloy. Hence, the relationships are based upon limited information obtained over a limited cyclic life range. The least squares curve fit life relationships should not be extrapolated much beyond the cyclic life range of the existing data. Although the scatter in the PP, PC, and CC data appears to be very small, this may simply be due to the few data points, since the scatter in the CP points is substantial. For example, test specimen numbers 20 and 23 (Table IV of Appendix 1) are essentially duplicate tests, yet the observed cyclic lives were 12 and 41 respectively. This spread of nearly 4 to 1 in observed life limits the ability of SRP, and for that matter, any high-temperature fatigue approach, to accurately correlate the behavior of this group of specimens. A measure of how well SRP can correlate the baseline results is given in Fig. 4(f). Correlation within life factors of two is obtained except, of course, for the 12 cycle CP test which had a predicted life of 45 cycles. Caution should be exercised in extrapolating EQ(2) to longer times to failure at temperatures on the order of 760°C and higher. The creep-formed powder processed alloy may begin to exhibit greater creep deformation due to superplasticity at longer times and low stresses which could result in improvements in the alloy's resistance to CP and CC type strainranges.

The amount of improvement could be evaluated from a knowledge of creep-rupture ductility and an application of the DN-SRP life estimation equations of Ref. 6. Unfortunately, no ductility data were available for this alloy at the relatively high temperature of 760°C.

Cast IN 100 - A set of SRP life relationships for cast IN 100 tested at 925°C were included in Ref. (5). These were based upon the preliminary data available at that time. A few of the originally tested specimens had failed prematurely at thermocouple spot welds, so these data points have been eliminated from the data base. Some additional tests were conducted on specimens with the thermocouples located further from the critical test section to avoid premature failures. The currently available data for 925°C although somewhat meager, are displayed in Figs. 5(a)-(e) along with the least squares curve fit life relationships.

Cast IN 100925°CLeast Squares Fit

$$\begin{aligned}
 \Delta \epsilon_{PP} &= 0.053(N_{PP})^{-0.57} \\
 \Delta \epsilon_{PC} &= 0.053(N_{PC})^{-0.73} \\
 \Delta \epsilon_{CP} &= 0.040(N_{CP})^{-0.55} \\
 \Delta \epsilon_{CC} &= 0.033(N_{CC})^{-0.44}
 \end{aligned}
 \quad \text{EQ (3)}$$

The few data exhibit little scatter for PC, CP, and CC. However, this may again be misleading as was suggested previously for the Gatorized IN 100, since there is scatter of very nearly a factor of two in the PP data. Correlation of the results is within factors of two on cyclic life as demonstrated in Fig. 5(f).

## Comparison With DN-SRP Equations

In a recently published paper (Ref.6) a set of equations was proposed which permits the estimation of the four SRP life relationships from a knowledge of a material's ductility. Referred to as the Ductility Normalized-Strainrange Partitioning (DN-SRP) equations, they were based upon a correlation of the SRP data available at the time of publication. All four inelastic strainrange components are related to life by power law equations with a constant exponent of -0.60. The coefficients in the equations are related to the ductility of the alloy at the temperature and in the environment of interest. Plastic ductility,  $D_p$ , as determined from percent reduction of area, R.A., obtained from conventional tensile tests, is used in the equations for PP and PC since these two types of strainranges have plasticity in the tensile half of the cycle. Similarly, creep-rupture ductility,  $D_c$ , is used in the expressions for CP and CC since creep strain is present in the tensile halves of these cycles. If creep-rupture ductility varies with time to failure, the DN-SRP equations imply that the CP and CC cyclic life relations are also a function of time. The DN-SRP life equations are as given below:

DN-SRPEQUATIONS

$$\begin{aligned}
 \Delta \epsilon_{PP} &= 0.50(D_p)(N_{PP})^{-0.60} \\
 \Delta \epsilon_{PC} &= 0.25(D_p)(N_{PC})^{-0.60} \\
 \Delta \epsilon_{CP} &= 0.20(D_c)(N_{CP})^{-0.60} \\
 \Delta \epsilon_{CC} &= 0.10(D_c)(N_{CC})^{-0.60}
 \end{aligned}
 \quad \text{EQ (4)}$$



There are two equations for CP. The first, with the 0.20 coefficient is for use when the creep-rupture cracking mode is transgranular. The latter is to be used when creep-rupture cracking is of the more detrimental intergranular mode.

Ductility data are available only for the uncoated Rene' 80 and the cast IN 100 alloys. However, implications of the DN-SRP equations with respect to the coated Rene' 80 will also be discussed.

Rene' 80 - Tensile ductility and creep-rupture ductility data for the uncoated Rene' 80 alloy are reported in Ref. (18) at several temperatures including 1000°C. For many alloys, the creep-rupture ductility decreases as rupture times become longer. This seems to be the case most frequently for alloys that crack in an intergranular mode. Rene' 80 is no exception in this regard. Creep-rupture cracking is intergranular. However, for the rupture times of interest (the same times as the failure times of the cyclic tests), the creep-rupture ductility,  $D_C$ , is essentially constant at a value of 0.17 over the time range from 2 to 150 hours to failure. The tensile plastic ductility is 0.60. Hence, the DN-SRP equations for uncoated Rene' 80 at 1000°C for a time span of up to 150 hours are:

$$\begin{aligned} \text{RENE' 80,} & \Delta \epsilon_{PP} = 0.200(N_{PP})^{-0.60} \\ \text{UNCOATED} & \Delta \epsilon_{PC} = 0.100(N_{PC})^{-0.60} \\ & \Delta \epsilon_{CP} = 0.034(N_{CP})^{-0.60} \\ & \Delta \epsilon_{CC} = 0.085(N_{CC})^{-0.60} \end{aligned} \quad \text{EQ (5)}$$

Equation (5) was used to predict the lives of the baseline tests for the uncoated Rene' 80. Fig. 6(a) compares the predicted lives with the observed lives. All but two of the points are within factors of three in cyclic life.

It was shown earlier that little difference exists between the behavior of the coated and uncoated specimens. This condition is attributed to at least two factors, (a) the coating is compatible with the base alloy and does not adversely affect its fatigue resistance as evidenced by the 1000°C vacuum data of Refs. 8 and 9, and (b) the current testing times (less than 150 hours), are not long enough for the uncoated specimens to experience life degradation due to oxidation, i.e., the protective capabilities of the coating are not as yet required. However, for exposure times much greater than 150 hours, uncoated Rene' 80 may suffer from oxidation attack whereas coated Rene' 80 would not do so under the same circumstances. One way to anticipate whether the SRP life relations would be altered by long exposure times is to evaluate the DN-SRP equations using ductility data obtained from tensile tests on exposed material and long time creep-rupture tests. The creep-rupture ductility,  $D_C = \ln [100/(100 - \%R.A.)]$ , of uncoated Rene' 80 in 1000°C air decreases from an average value of 0.17 in the 2 to 150 hour regime to 0.11 at 1000 hours to rupture.

We would thus expect the CP and CC SRP life relationships for uncoated Rene' 80 appropriate for 1000 hour lives to decrease in accordance with the decrease in  $D_C$  as indicated by the DN-SRP relations of Eq. (4). No plastic ductility data were available for uncoated material that had been exposed for long periods of time, nor were any ductility data available for the coated material. Hence, we can not presently evaluate whether the long time SRP life relations for the coated and uncoated material would be expected to differ or remain the same. The above discussion, however, does suggest how such an evaluation could be made without resorting to expensive long time cyclic tests.

Cast IN 100 - Ductility data for the cast IN 100 alloy were reported in Ref. 18. For the 925°C test temperature and failure times of less than 100 hours, the corresponding ductilities are:  $D_p = D_C = 0.11$ , with intergranular cracking being responsible for the creep-rupture failures. Hence, for these conditions, the DN-SRP equations for cast IN 100 at 1000°C are:

$$\begin{aligned} \text{CAST IN 100} & \Delta \epsilon_{PP} = 0.055(N_{PP})^{-0.60} \\ & \Delta \epsilon_{PC} = 0.028(N_{PC})^{-0.60} \\ & \Delta \epsilon_{CP} = 0.025(N_{CP})^{-0.60} \\ & \Delta \epsilon_{CC} = 0.063(N_{CC})^{-0.60} \end{aligned} \quad \text{EQ (6)}$$

Figure 6(b) compares the predicted lives of the cast IN 100 with the observed baseline lives. All of the data are contained within factors of three of the predicted lives, and nearly all within factors of two.

#### Verification Results

Verification tests designed to check the predictive capability of the SRP life equations were conducted only with specimens of cast IN 100, since sufficient specimens were simply unavailable for the other alloys. A primary requisite of a verification test is that it should contain some feature or complexity not present in the baseline test. For the present purposes, we selected an unusual strain-cycling test which contains periods of multiple stress relaxation as opposed to the baseline tests which contained periods of creep at constant stress. The process of determining the amounts of tensile and compressive creep and plasticity is straightforward. Referring to Fig. 2, the creep strain was determined from the amount of elastic strain converted to creep strain during each relaxation period. The plastic strain is the difference between the inelastic strain and the creep strain. For example, during the compressive portion of the multiple tensile relaxation cycle (MTRC) of Fig. 2(c), the compressive creep strain,  $\epsilon_{C1}$ , is equal to the amount of relaxed stress ( $\sigma_a - \sigma_b$ ) divided by the modulus of elasticity,  $E$ .

The compressive plastic strain is simply the difference between the inelastic strainrange  $\Delta\epsilon_{IN}$  and  $\epsilon_{C1}$ . In tension, there are three creep strain contributions,  $\epsilon_{C2}$ ,  $\epsilon_{C3}$ , and  $\epsilon_{C4}$ . Each is given by the amount of stress relaxation ( $\sigma_c - \sigma_d$ ), ( $\sigma_e - \sigma_f$ ), and ( $\sigma_g - \sigma_h$ ) divided by the elastic modulus. The tensile plastic strain is given by  $\Delta\epsilon_{IN} = (\epsilon_{C2} + \epsilon_{C3} + \epsilon_{C4})$ . Procedures for determining the partitioned inelastic strainrange components are given in Ref. 5. For the MTRC example, three strainrange components are present, PP, CP, and CC. For a multiple compressive relaxation cycle (MCRC), PP, PC, and CC strainrange components are introduced.

For each verification test conducted, the inelastic strainrange was used to calculate the respective NPP, NPC, NCP, and NCC lives from the least squares curve fit life relations of EQ. (3). Knowing the partitioned inelastic strainrange components permitted calculation of the strainrange fractions, FPP, FPC, FCP, and FCC for use in the interaction damage rule so that the predicted cyclic lives NPRED could be computed.

$$(FPP/NPP) + (FPC/NPC) + (FCP/NCP) + (FCC/NCC) = 1/NPRED \quad EQ (7)$$

A series of three MTRC and three MCRC tests were conducted with the cast IN 100 at 925°C using the six minute cycle illustrated schematically in Fig. 2. Table IV of Appendix 1 lists the pertinent data for each verification test. Comparisons of the observed lives and predicted lives are presented in Fig. 8. It is seen that cyclic lives were predicted to within factors of two in every case.

#### SUMMARY AND CONCLUDING REMARKS

In keeping with the objectives of this Specialists Meeting, this paper focused on an evaluation of how well the Method of Strainrange Partitioning (SRP) can both correlate and predict the high-temperature, low-cycle fatigue lives of laboratory specimens of advanced gas turbine alloys.

Strainrange Partitioning characteristics were presented for two nickel-base superalloys: cast Rene' 80 with and without an aluminide (Codep B-1) coating, and IN 100 in both the Gatorized (creep-formed) and cast conditions. SRP life relationships were established for each of the four inelastic strainrange types (PP, PC, CP, and CC) for each alloy condition.

By comparing the observed lives of the baseline tests with the lives calculated from the established life relationships, it was shown that the method of Strainrange Partitioning successfully correlated the high-temperature, low-cycle fatigue lives of these alloys generally to within factors of two. It should, of course, be kept in mind that the SRP inelastic strainrange versus life relationships for the cast nickel-base superalloys studied in this program are not widely separated one from another. These circumstances are believed to result from the fact that these alloys were designed to resist creep deformation by the prevention of grain boundary sliding, a mechanism frequently associated with widely separated CP and PP SRP life relationships.

An evaluation was also made of how well the recently proposed Ductility Normalized-Strainrange Partitioning (DN-SRP) equations could predict the cyclic lives of the baseline tests. Values of tensile plastic ductility,  $D_p$ , and creep-rupture ductility,  $D_c$ , for use in the DN-SRP equations were determined at the temperature and failure times corresponding to the baseline data, and then used to determine the PP, PC, CP, and CC life relationships. These life relationships were then applied, in conjunction with the interaction damage rule to predict the cyclic lives of the baseline tests. Agreement between predicted and observed lives was generally within factors of 3. Only uncoated Rene' 80 and cast IN 100 were evaluated since ductility data were unavailable for the other conditions of these alloys.

A few verification type tests were conducted on specimens of cast IN 100 using a test cycle composed of hold periods at several different constant strain levels. Creep was thereby introduced into each cycle by the process of repeated stress relaxation. One series of tests was conducted which featured three hold periods in tension and a much shorter period at the peak compressive strain, thus producing partitioned inelastic strainrange components of CP, CC, and PP. Another series of tests reversed the holding pattern of strain and thus gave rise to PC, CC, and PP components. The lives of the verification tests were predicted on the basis of the life relationships established from the baseline tests which had introduced creep in a more direct manner by using hold periods at constant stress. The life of each verification test was predicted correctly to within factors of two, which is considered to be an acceptably high degree of predictability.

It is concluded that the method of Strainrange Partitioning can be used to accurately correlate and predict the high-temperature, low-cycle fatigue behavior of the nickel-base superalloys studied in this program.

#### REFERENCES

1. Manson, S.S.; Halford, G.R.; and Hirschberg, M.H.: Creep-Fatigue Analysis by Strain-Range Partitioning. Symposium on Design for Elevated Temperature Environment. ASME, 1971, pp. 12-28.
2. Manson, S.S.: A Review of the Development of Strainrange Partitioning. Proceedings, Characterization of Low Cycle High Temperature Fatigue by the Strainrange Partitioning Method, Sponsored by the AGARD Structures and Materials Panel, Aalborg, Denmark, April 1978.
3. Manson, S.S.: The Challenge to Unify Treatment of High Temperature Fatigue - A Partisan Proposal Based on Strainrange Partitioning. STP 520, ASTM, 1973, pp. 744-782.
4. Manson, S.S.: Observations and Correlations Emphasizing Wave Shape and Other Salient Features. Chapter 4, Time-Dependent Fatigue of Structural Alloys. A General Assessment (1975). ORNL-5073, Oak Ridge National Laboratory, January 1977, pp. 155-332.



5. Mirschberg, M.H.; and Halford, G.R.: Use of Strainrange Partitioning to Predict High-Temperature Low-Cycle Fatigue Life. NASA TN D-8072 1976.
6. Halford, G.R.; Saltsman, J.F.; and Mirschberg, M.H.: Ductility Normalized-Strainrange Partitioning Life Relations for Creep-Fatigue Life Prediction. Proceedings of the Conference on Environmental Degradation of Engineering Materials. Virginia Tech. Printing Dept., V.P.I. & State Univ., Blacksburg, VA 1977, pp. 599-612.
7. Mirschberg, M.H.: A Low-Cycle Fatigue Testing Facility. Manual on Low-Cycle Fatigue Testing. STP-465, ASTM, 1969, pp.67-86.
8. Kortovich, C.S.: Ultrahigh Vacuum, High Temperature, Low Cycle Fatigue of Coated and Uncoated Rene' 80. NASA CR-135003, April 1976. (TRW Inc., ER-7861).
9. Kortovich, C.S.; and Sheinker, A.A.: A Strainrange Partitioning Analysis of Low Cycle Fatigue of Coated and Uncoated Rene' 80. Proceedings, Characterization of Low Cycle, High Temperature Fatigue by the Strainrange Partitioning Method. Sponsored by the AGARD Structures and Materials Panel, Aalborg, Denmark, April 1978.
10. Wallace, R.M; Annis, G.G.; and VanWanderham, M.C.: Low Cycle Fatigue Behavior of IN 100: Strainrange Partitioning Method. Proceedings, Characterization of Low Cycle High Temperature Fatigue by the Method of Strainrange Partitioning. Sponsored by the AGARD Structures and Materials Panel, Aalborg, Denmark, April 1978.
11. Coffin, L.F., Jr.: Observations and Correlations Emphasizing Frequency and Environmental Effects. Chapter 3, Time-Dependent Fatigue of Structural Alloys. A General Assessment(1975). ORNL-5073, Oak Ridge National Laboratory, January 1977, pp.37-153.
12. Ostergren, W.J.: Correlation of Hold Time Effects in Elevated Temperature Low Cycle Fatigue Using A Frequency Modified Damage Function. 1976 ASME-MPC Symposium on Creep-Fatigue Interaction, MPC-3, December 1976, pp. 179-202.
13. Ellis, J.R.; and Esztergar, E.P.: Consideration of Creep-Fatigue Interaction in Design Analysis. Symposium on Design for Elevated Temperature Environment, ASME, 1971, pp. 29-43.
14. Majumdar, S.; and Maiya, P.S.: A Damage Equation for Creep-Fatigue Interaction. 1976 ASME-MPC Symposium on Creep-Fatigue Interaction, MPC-3, December 1976, pp. 323-335.
15. Spera, D.A.: The Calculation of Elevated-Temperature Cyclic Life Considering Low-Cycle Fatigue and Creep. NASA TN D-5317, 1969.
16. Manson, S.S.; Halford, G.R.; and Spera, D.A.: The Role of Creep in High-Temperature Low-Cycle Fatigue. Ch. 12 in Advances in Creep Design. A.I.Smith and A.M.Nicolson, eds., Appl. Sci Publ.Ltd. London, 1971, pp. 229-249.
17. Section III, Boiler and Pressure Vessel Code, Code Case 1592, ASME, 1977.
18. Fritz, L.J.; and Koster, W.P.: Tensile and Creep Rupture Properties of 16 Uncoated and 2 Coated Engineering Alloys at Elevated Temperatures. NASA CR-135138, METCUT Research Associates, Inc.1977.

ORIGINAL PAGE IS  
OF POOR QUALITY

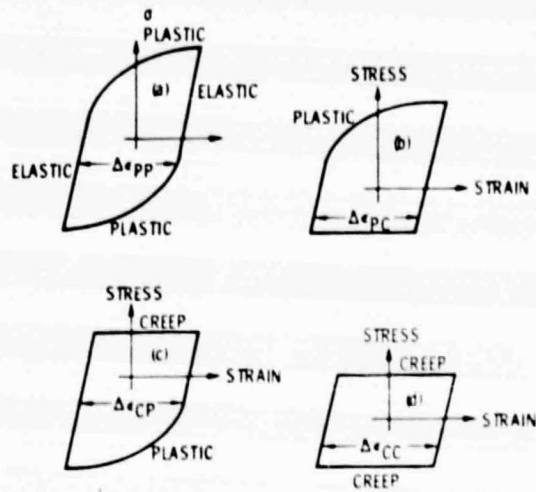


Figure 1. - Schematic illustration of hysteresis loops resulting from test cycles used to establish baseline strainrange partitioning life relationships for Rene® 80, Gatorized IN 100, and cast IN 100.

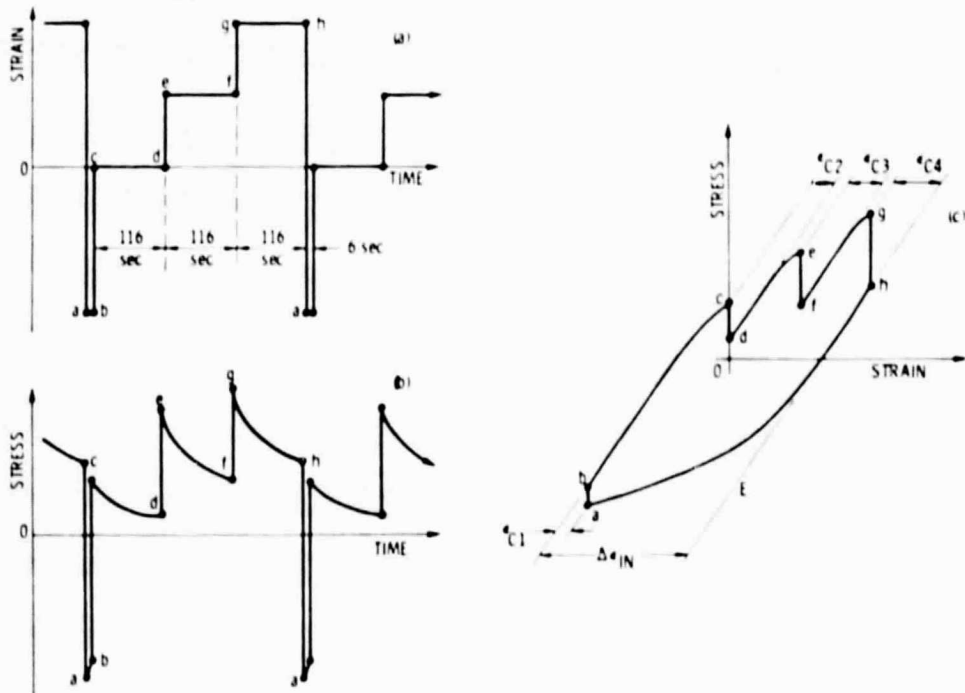


Figure 2. - Schematic representation of verification test cycle involving multiple strain hold periods. Multiple Tensile Relaxation Cycle (MTRC) shown. (a) Programmed strain-time waveform, (b) Stress-time response, and (c) Stress-strain hysteresis loop.

ORIGINAL PAGE IS  
OF POOR QUALITY

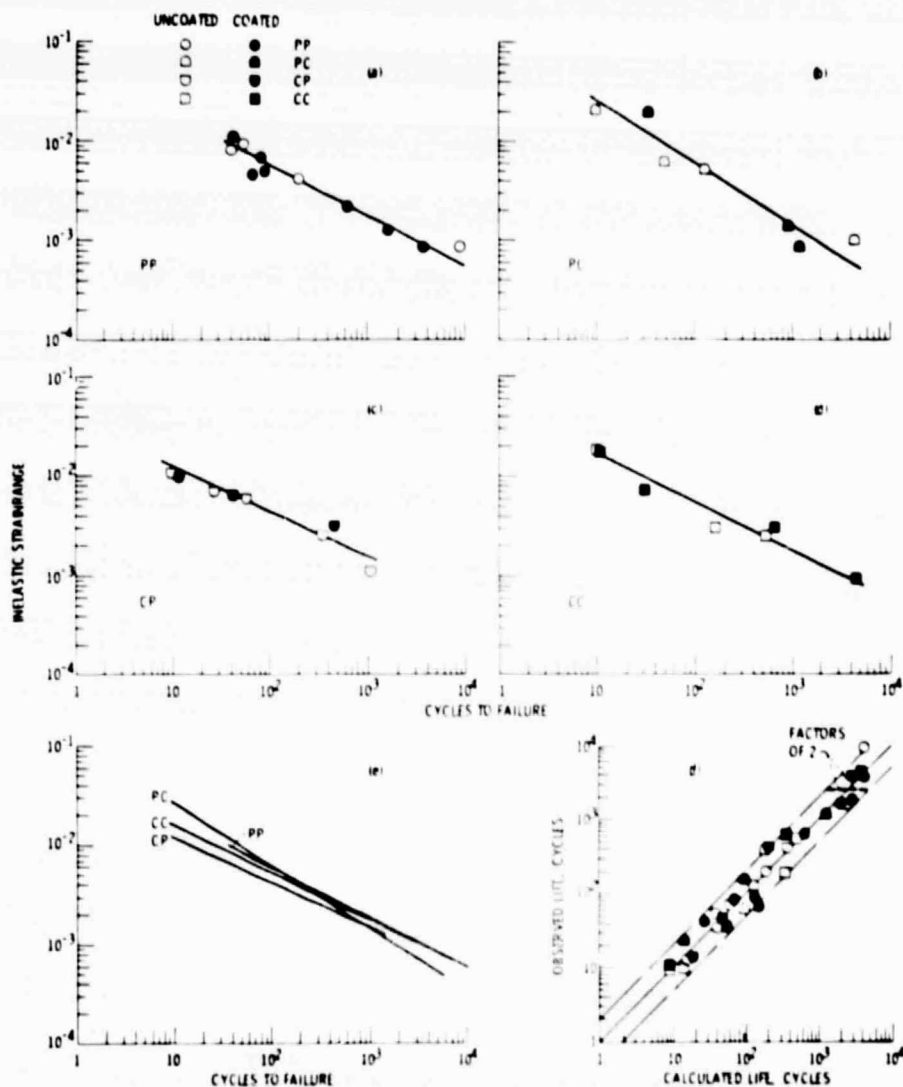


Figure 3 - Strainrange partitioning life relationships for cast Rene 80 with and without Codep B-1 aluminate coating in air at  $1000^{\circ}\text{C}$ . Least squares curve fit of baseline data. Note little difference between coated and uncoated behavior. (a) PP life relationship, (b) PL life relationship, (c) CP life relationship, (d) CC life relationship, (e) Superposition of life relationships, and (f) Life relationships correlate baseline data to within factors of 2 in cyclic life.

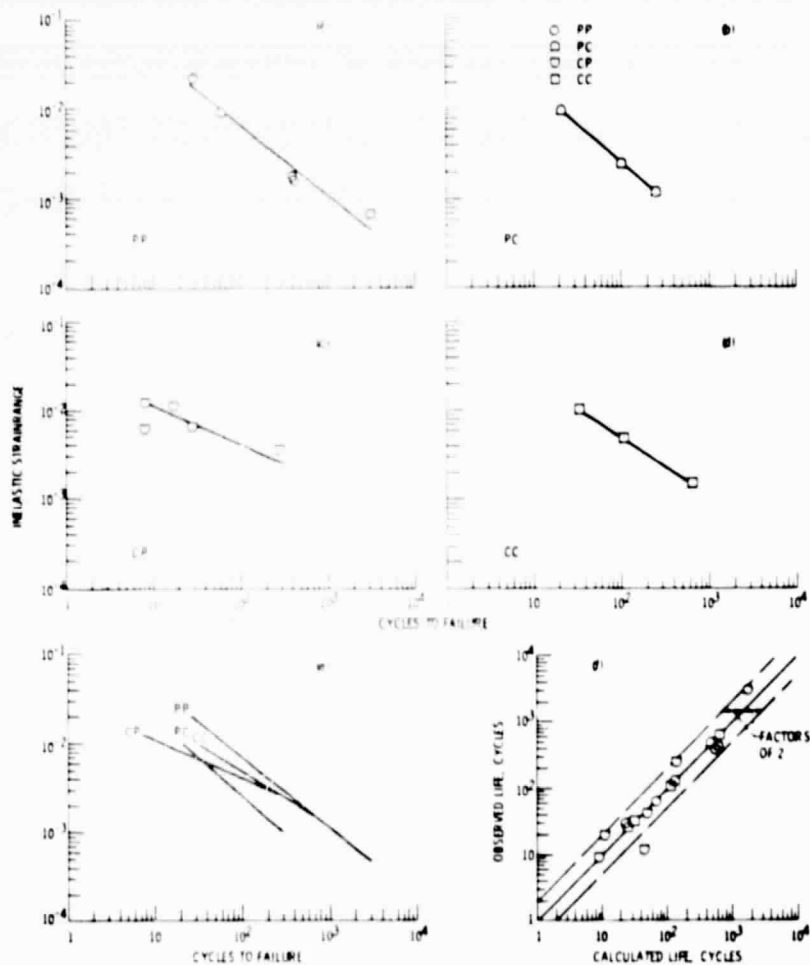


Figure 4. - Strainrange partitioning life relationships for Lakeview IN 100 in air at 760°C. Least squares curve fit of baseline data.  
 (a) PP life relationship, (b) PC life relationship, (c) CP life relationship, (d) CC life relationship, (e) Superposition of life relationships, and (f) Life relationships correlate baseline data generally within factors of 2 in cyclic life.

ORIGINAL PAGE IS  
OF POOR QUALITY

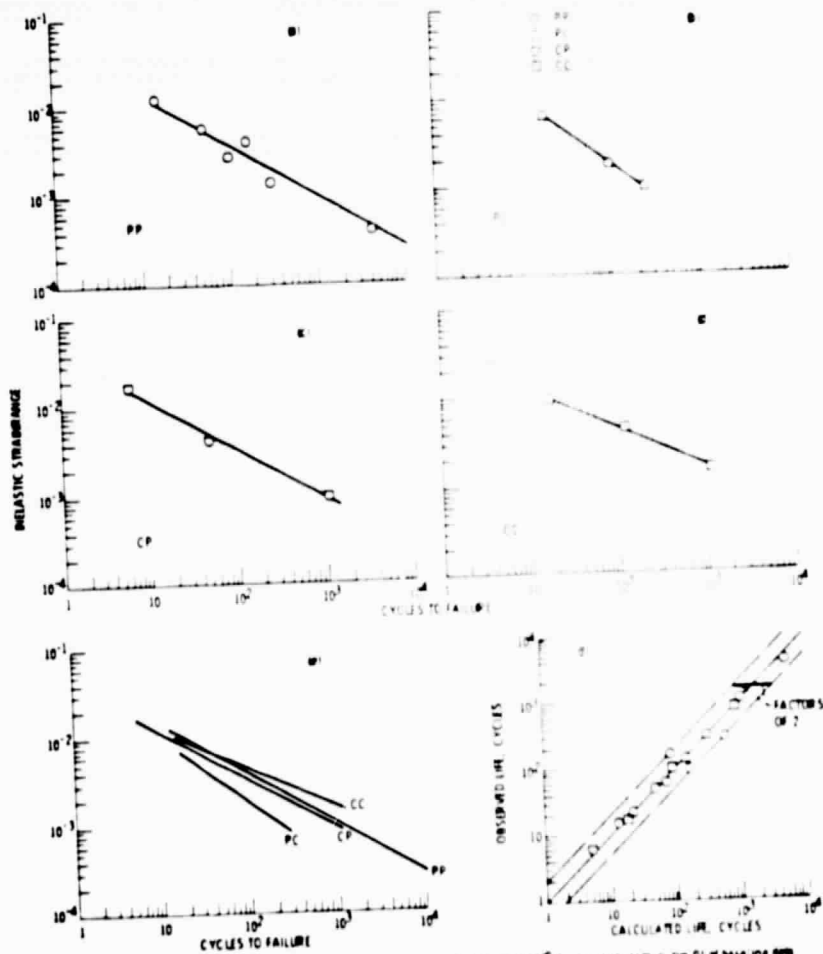
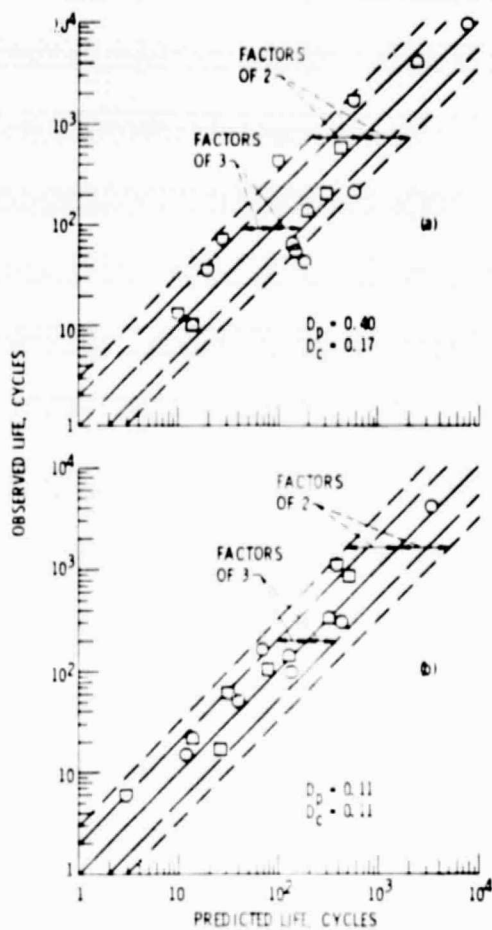


Figure 5 - Strainrange partitioning life relationships for cast 14-100 in air at 600°C. Least squares curve fit of baseline data: (a) PP life relationship; (b) PC life relationship; (c) CC life relationship; (d) PP life relationship; (e) PC life relationship; (f) comparison of life relationships, and (f) life relationships correlate baseline data to within factors of 2 in cyclic life.





**ORIGINAL PAGE IS  
OF POOR QUALITY**

Figure 6. - Application of the ductility normalized-strainrange partitioning life equations to the prediction of the baseline data. (a) René 80, uncoated, 1000°C, and (b) Cast IN 100, 925°C.

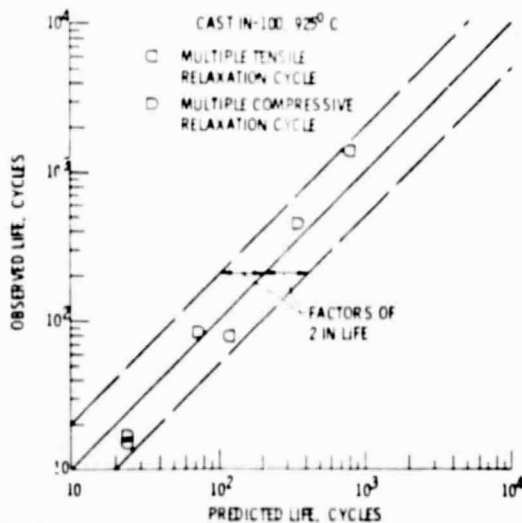


Figure 7. - Strainrange partitioning predicts lives of multiple strain hold time verification tests to within factors of two.

## APPENDIX 1 - MATERIAL DATA SUMMARY

TABLE I: CHEMICAL COMPOSITION - WT %

MATERIAL	Al	Si	B	C	Co	Ti	V	W	Cr	Zr	Fe	Mo	Mn	Ni
RENE' 80	2.990	<0.050	0.015	0.170	9.730	4.870	-----	3.940	13.800	0.043	0.130	4.110	<0.020	BAL
IN 100 (GATORIZED)	4.980	-----	0.020	0.070	18.500	4.320	0.780	-----	12.400	0.060	-----	3.200	-----	BAL
IN 100 (CAST)	5.450	0.110	0.016	0.170	15.100	4.760	0.970	-----	10.300	0.084	-----	2.960	0.020	BAL

TABLE II: PROCESSING &amp; HEAT TREATMENT

MATERIAL	PROCESSING	HEAT TREATMENT
Rene' 80	TRW master heat no. BL-5138, bare & coated with Codep B-1(aluminide). Individually cast bars (hole bored for tubular specimens). ASTM grain size = 3.	1220C-2hr. in vac., inert Q to RT; 1095C-4hr. in vac., inert Q to RT; 1050C-4hr. in vac., FC in 1 hr. to 650C, AC to RT (simulates coating cycle); 845C-16hr. in vac., FC to RT. Rough machine before heat treatment, finish grind after.
IN 100	Powder - GATORIZED(TM)	Solution 2050F, Stabilized 1600F and 1800F, precipitation 1200F and 1400F.
IN 100	CAST	None

TABLE III: MECHANICAL PROPERTIES  
(1MPa = 0.145KSI)

MATERIAL	TENSILE PROPERTIES					CREEP-RUPTURE PROPERTIES					
	TEMP C	MODULUS MPa	0.2% YIELD MPa	ULTIMATE MPa	RA-%	10 HR		100 HR		1000 HR	
						MPa	RA-%	MPa	RA-%	MPa	RA-%
RENE' 80	20	198,600	821.0	996.0	6.2						
	1000	128,200	230.0	333.0	32.7	180.0	16.5	127.6	12.5	82.7	10.5
IN 100 (CAST)	20	205,500	866.0	1040.0	12.1						
	925	155,100	467.0	622.0	10.2	430.0	10.3	262.0	10.3	158.6	10.3

ORIGINAL PAGE IS  
OF POOR QUALITY

TABLE IV - CREEP-FATIGUE DATA

Spec. No. RES-	Test Type	Freq. Hz	Stress at $N_f/2$ , MPa			Strainrange at $N_f/2$ , %							Cycles to Failure, $N_f$	Hours to Failure, $t_f$
			Tens. Max.	Comp. Max.	Range	Total	Elastic	Inelastic	PP	PC	CP	CC		
Resor 80, Uncoated, 1000°C														
205	PP	1.00-00	620.9	620.9	641.8	1.525	0.454	0.469	0.069	0.000	0.000	0.000	42	0.01
210		1.00-00	370.0	370.0	741.0	1.557	0.570	0.579	0.079	0.000	0.000	0.000	55	0.01
206		1.00-00	350.2	350.2	710.4	0.909	0.550	0.431	0.431	0.000	0.000	0.000	202	0.06
204		1.00-00	206.2	206.2	412.4	0.010	0.721	0.009	0.009	0.000	0.000	0.000	9236	2.06
200	PC	6.00-05	447.1	170.3	640.6	2.612	0.504	2.100	0.222	1.066	0.000	0.000	10	00.75
219		7.00-04	355.0	136.0	691.0	1.007	0.303	0.620	0.260	0.356	0.000	0.000	63	23.33
213		9.00-06	321.7	170.9	501.2	0.016	0.301	0.525	0.250	0.267	0.000	0.000	132	36.64
210		7.00-03	103.3	110.7	303.0	0.339	0.237	0.102	0.021	0.071	0.000	0.000	3900	105.00
223	CP	6.00-05	127.7	405.7	533.4	1.672	0.416	1.056	0.299	0.000	0.757	0.000	13	56.00
200		5.00-04	172.6	301.0	516.0	1.090	0.400	0.690	0.210	0.000	0.400	0.000	25	17.97
201		5.50-04	172.0	276.7	448.7	0.927	0.350	0.577	0.195	0.000	0.382	0.000	70	35.63
221		6.20-03	110.0	250.2	360.6	0.536	0.201	0.253	0.089	0.000	0.164	0.000	616	27.26
220	CC	2.20-02	89.0	225.6	316.6	0.350	0.245	0.109	0.055	0.000	0.054	0.000	1600	19.05
211		1.00-03	206.1	206.1	400.3	2.216	0.381	1.833	0.276	0.000	0.000	1.557	10	1.56
212		6.20-04	157.0	134.2	293.2	0.531	0.228	0.303	0.071	0.000	0.000	0.232	191	65.10
217		9.20-03	156.3	112.7	269.0	0.461	0.211	0.250	0.067	0.000	0.000	0.103	500	16.60
Resor 80, Coated, 1000°C														
322	PP	1.00-00	601.5	601.5	1203.0	1.917	0.751	1.166	1.166	0.000	0.000	0.000	43	0.01
317		1.00-00	394.6	394.6	789.2	1.091	0.615	0.476	0.476	0.000	0.000	0.000	60	0.32
310		1.00-00	600.0	600.0	1200.0	1.399	0.607	0.712	0.712	0.000	0.000	0.000	65	0.32
308		1.00-00	375.2	375.2	750.4	1.101	0.505	0.516	0.516	0.000	0.000	0.000	93	0.03
306	PC	1.00-00	290.6	230.6	597.2	0.696	0.465	0.231	0.231	0.000	0.000	0.000	650	0.10
307		1.00-00	239.5	239.5	479.0	0.515	0.365	0.130	0.130	0.000	0.000	0.000	1666	0.66
309		1.00-00	190.2	190.2	380.4	0.397	0.309	0.088	0.088	0.000	0.000	0.000	3020	1.06
305		1.00-00	170.2	170.2	340.4	0.226	0.270	0.046	0.046	0.000	0.000	0.000	15003	0.20
304	CP	5.00-04	365.6	170.1	563.7	2.410	0.424	1.986	0.330	1.656	0.000	0.000	26	13.20
301		2.20-03	323.5	172.7	496.2	1.007	0.387	0.620	0.224	0.392	0.000	0.000	159	20.67
303		3.00-03	216.1	86.0	310.9	0.387	0.248	0.139	0.063	0.076	0.000	0.000	1200	97.25
320		1.30-01	210.1	77.3	287.4	0.312	0.224	0.080	0.044	0.044	0.000	0.000	1900	0.10
315	CC	9.10-04	164.1	353.2	522.3	1.369	0.407	0.962	0.234	0.000	0.724	0.000	10	0.25
305		1.10-03	102.9	302.9	502.0	1.022	0.392	0.630	0.114	0.000	0.496	0.000	40	11.00
308		1.00-03	100.0	298.7	398.7	0.631	0.311	0.320	0.008	0.000	0.232	0.000	432	63.67
302		1.10-03	90.3	210.6	300.9	0.337	0.235	0.102	0.050	0.000	0.044	0.000	3020	65.65
309	CC	5.00-04	203.1	236.9	440.0	2.133	0.343	1.790	0.342	0.000	0.000	1.448	11	5.62
316		6.00-04	169.1	165.3	334.4	0.904	0.261	0.723	0.141	0.000	0.036	0.546	35	20.68
313		2.60-02	115.9	136.1	252.0	0.492	0.197	0.295	0.105	0.000	0.000	0.260	620	65.23
314		6.00-02	103.0	110.3	221.7	0.266	0.173	0.093	0.011	0.000	0.000	0.002	4457	25.92
Galvanized DN 100, 760°C														
9	PP	0.00-01	1305.0	1510.0	2823.0	3.424	1.637	2.287	2.287	0.000	0.000	0.000	29	0.01
17		0.00-01	1170.0	1190.0	2360.0	2.305	1.373	0.933	0.933	0.000	0.000	0.000	63	0.02
19		0.00-01	952.0	907.0	1859.0	1.256	1.077	0.179	0.179	0.000	0.000	0.000	401	0.10
12		0.00-01	910.0	910.0	1820.0	1.222	1.057	0.165	0.165	0.000	0.000	0.000	413	0.15
8	PC	0.00-01	670.0	660.0	1330.0	0.895	0.776	0.069	0.069	0.000	0.000	0.000	3005	1.07
6		2.50-06	1117.0	433.0	1550.0	1.892	0.899	0.993	0.273	0.720	0.000	0.000	36	20.00
13		6.70-03	800.0	215.0	1019.0	0.826	0.591	0.230	0.072	0.166	0.000	0.000	129	51.70
10		6.00-03	620.0	430.0	1050.0	0.736	0.617	0.119	0.083	0.036	0.000	0.000	503	30.60
18	CP	1.00-00	699.0	1270.0	1770.0	2.240	1.029	1.212	0.192	0.000	1.020	0.000	9	17.75
20		7.00-06	560.0	1161.0	1721.0	1.633	0.999	0.634	0.204	0.000	0.430	0.000	12	6.70
15		7.10-06	317.0	1163.0	1480.0	1.760	0.340	1.140	0.212	0.000	0.920	0.000	20	7.60
23		1.00-03	662.0	1205.0	1867.0	1.710	1.082	0.636	0.276	0.000	0.360	0.000	61	7.00
6	CC	5.00-03	553.0	1050.0	1603.0	1.299	0.920	0.371	0.091	0.000	0.200	0.000	290	12.30
22		7.10-06	670.0	699.0	1369.0	1.754	0.791	0.973	0.193	0.000	0.000	0.736	33	12.00
3		3.00-03	600.0	623.0	1223.0	1.192	0.715	0.477	0.101	0.000	0.000	0.200	112	0.26
16	CC	1.70-02	521.0	521.0	1042.0	0.755	0.604	0.151	0.022	0.000	0.002	0.127	652	16.00
Cast DN 100, 826°C														
2	PP	5.00-01	730.0	770.0	1510.0	2.170	0.924	1.246	1.246	0.000	0.000	0.000	15	0.31
32		5.00-01	573.0	619.2	1192.0	1.351	0.749	0.502	0.502	0.000	0.000	0.000	50	3.33
3		5.00-01	803.0	520.0	1003.0	0.920	0.630	0.292	0.292	0.000	0.000	0.000	96	0.05
17		5.00-01	500.7	500.1	1112.0	1.125	0.700	0.417	0.417	0.000	0.000	0.000	160	0.11
10	PC	5.00-01	305.3	609.7	706.0	0.600	0.500	0.100	0.100	0.000	0.000	0.000	200	0.17
36		5.00-01	324.1	220.2	452.3	0.332	0.292	0.040	0.040	0.000	0.000	0.000	4015	2.23
20		5.00-01	172.0	172.0	345.0	0.236	0.222	0.016	0.016	0.000	0.000	0.000	51201	20.36
74	CP	5.10-06	500.7	261.3	766.0	1.324	0.481	0.643	0.207	0.436	0.000	0.000	22	12.02
13		0.00-00	806.0	180.6	627.4	0.577	0.399	0.170	0.076	0.102	0.000	0.000	130	07.31
15		7.10-06	612.3	181.3	553.6	0.450	0.352	0.098	0.030	0.064	0.000	0.000	332	129.11
90	CC	2.70-04	322.7	670.3	997.0	2.300	0.443	1.457	0.149	0.000	1.200	0.000	6	6.09
11		1.00-03	169.6	590.3	761.9	0.899	0.405	0.414	0.182	0.000	0.232	0.000	60	153.02
9		1.00-03	170.0	360.6	502.6	0.416	0.220	0.096	0.067	0.000	0.007	0.000	1100	150.32
12	CC	1.00-05	220.2	220.2	440.0	1.208	0.290	0.918	0.108	0.000	0.000	0.010	17	101.50
16		1.00-04	171.0	171.0	342.0	0.451	0.210	0.432	0.019	0.019	0.000	0.174	102	202.37
09		3.00-03	200.7	200.7	401.0	0.402	0.250	0.150	0.065	0.000	0.000	0.000	000	70.33
73	VERIF	2.00-03	621.5	655.0	1276.5	1.625	0.823	0.802	0.673	0.107	0.000	0.010	17	1.73
72		2.00-03	366.1	355.1	721.2	0.822	0.465	0.357	0.210	0.105	0.000	0.033	84	0.60
67		2.00-03	365.0	259.2	604.6	0.517	0.390	0.127	0.054	0.043	0.000	0.030	690	07.11
75	VERIF	2.00-03	436.0	502.6	1019.0	1.502	0.657	0.845	0.724	0.000	0.000	0.022	15	1.55
60		2.00-03	375.1	662.6	817.7	0.806	0.560	0.246	0.181	0.000	0.132	0.013	79	7.07
66		2.00-03	267.5	352.0	599.0	0.505	0.367	0.138	0.053	0.000	0.000	0.021	1400	140.07

TABLE IV - CREEP-FATIGUE DATA

Spec. No. REE-	Test Type	Freq. Hz	Stress at $N_f/2$ , MPa		Strainrange at $N_f/2$ , %						Cycles to Failure, $N_f$	Hours to Failure, $t_f$	
			Tens. Max.	Comp. Range Max.	Total	Elastic	Inelastic	PP	PC	CP			CC
Rene <sup>®</sup> 80, Uncoated, 1000°C													
202	PP	1.0E-00	420.9	420.3	841.4	1.525	0.556	0.459	0.000	0.000	0.000	42	0.01
215		1.0E-00	370.9	370.9	741.4	1.557	0.578	0.479	0.000	0.000	0.000	45	0.01
206		1.0E-00	356.2	356.2	716.4	0.969	0.558	0.431	0.000	0.000	0.000	202	0.06
204		1.0E-00	206.2	206.2	412.4	0.410	0.321	0.049	0.000	0.000	0.000	9226	2.46
200	PC	6.8E-05	457.1	173.3	644.4	2.612	0.504	2.104	0.222	1.466	0.000	10	40.75
219		7.0E-04	355.0	136.0	491.0	1.007	0.483	0.524	0.268	0.456	0.000	63	23.53
211		9.8E-04	321.7	174.5	501.2	0.916	0.491	0.525	0.258	0.267	0.000	132	36.64
213		7.6E-03	183.3	119.7	303.0	0.339	0.237	0.102	0.031	0.071	0.000	3980	145.00
223	CP	6.4E-05	127.7	405.7	533.4	1.472	0.416	1.056	0.249	0.000	0.757	13	55.00
208		5.4E-04	172.6	341.4	514.0	1.094	0.400	0.698	0.218	0.000	0.480	35	17.97
201		5.5E-04	172.0	276.7	448.7	0.927	0.350	0.577	0.195	0.000	0.382	70	35.63
221		4.2E-03	110.4	250.2	360.6	0.534	0.281	0.253	0.049	0.000	0.164	816	27.26
220		2.2E-02	89.0	225.6	314.6	0.354	0.245	0.103	0.055	0.000	0.054	1500	13.35
224		1.8E-03	244.1	244.1	488.2	1.472	0.416	1.056	0.249	0.000	0.757	13	55.00
231	CC	1.8E-03	244.1	244.1	488.2	1.472	0.416	1.056	0.249	0.000	0.757	13	1.56
212		6.2E-04	587.8	135.2	723.0	0.531	0.228	0.303	0.071	0.000	0.232	191	95.10
217		9.2E-03	156.3	112.7	269.0	0.461	0.211	0.250	0.107	0.000	0.183	548	16.60
Rene <sup>®</sup> 80, Coated, 1000°C													
122	PP	1.0E-00	491.5	491.5	983.0	1.917	0.751	1.166	1.166	0.000	0.000	43	3.01
117		1.0E-00	394.6	394.6	789.2	1.091	0.615	0.476	0.676	0.000	0.000	69	3.32
110		1.0E-00	440.4	440.4	880.8	1.193	0.687	0.506	0.712	0.000	0.000	85	3.72
104		1.0E-00	375.2	375.2	750.4	1.101	0.585	0.516	0.516	0.000	0.000	93	3.03
106		1.0E-00	248.6	248.6	497.2	0.696	0.465	0.231	0.000	0.000	0.000	650	3.19
100		1.0E-00	219.5	219.5	439.0	0.515	0.385	0.130	0.130	0.000	0.000	1565	4.46
123		1.0E-00	198.2	198.2	396.4	0.397	0.309	0.088	0.048	0.000	0.000	3823	1.36
111		1.0E-00	178.2	178.2	356.4	0.324	0.278	0.046	0.046	0.000	0.000	15303	4.28
112	PC	5.0E-04	365.6	173.1	543.7	2.410	0.424	1.966	0.310	1.556	0.000	24	13.20
101		2.2E-03	323.5	172.7	496.2	1.007	0.387	0.620	0.228	0.392	0.000	153	20.47
103		3.8E-03	234.1	144.9	379.0	0.367	0.248	0.119	0.083	0.076	0.000	1200	97.25
128		1.3E-01	210.1	77.3	287.4	0.312	0.224	0.088	0.044	0.044	0.000	1903	4.10
115	CP	9.1E-04	165.1	151.2	316.3	1.169	0.407	0.762	0.215	0.600	0.724	14	4.25
105		1.1E-01	152.9	144.9	297.8	1.032	0.392	0.640	0.114	0.496	0.000	44	11.68
104		1.1E-01	100.0	218.7	318.7	0.631	0.311	0.320	0.044	0.000	0.232	432	43.47
102		1.1E-01	90.3	210.6	300.9	0.337	0.235	0.102	0.054	0.000	0.044	3924	45.45
109	CC	1.8E-03	201.1	235.9	443.0	2.113	0.343	1.770	0.342	0.000	0.000	11	5.62
116		4.2E-04	169.1	165.3	334.4	0.934	0.261	0.673	0.143	0.000	0.034	35	20.44
113		2.2E-03	115.9	115.1	231.0	0.472	0.197	0.295	0.035	0.000	0.000	620	65.23
114		4.8E-03	103.4	118.3	221.7	0.266	0.173	0.093	0.011	0.000	0.082	4457	25.32

TABLE IV - CREEP-FATIGUE DATA(Cont.)

Spec. No. INN-	Test Type	Freq. Hz	Stress at $N_f/2$ , MPa		Strainrange at $N_f/2$ , %						Cycles to Failure, $N_f$	Hours to Failure, $t_f$		
			Tens. Max.	Comp. Max.	Range	Total	Elastic	Inelastic	PP	PC			CP	CC
Gatorized IN 100, 760°C														
9		8.0E-01	1305.0	1519.0	2423.0	3.424	1.017	2.287	2.287	0.000	0.000	0.000	23	9.21
17	PP	8.0E-01	1170.0	1194.0	2364.0	2.355	1.373	0.933	0.933	0.000	0.000	0.000	63	3.02
19		8.0E-01	952.0	907.0	1859.0	1.456	1.077	0.179	0.179	0.000	0.000	0.000	401	0.14
12		8.0E-01	914.0	914.0	1828.0	1.222	1.057	0.165	0.165	0.000	0.000	0.000	413	0.15
8		8.0E-01	670.0	665.0	1366.0	0.845	0.776	0.063	0.063	0.000	0.000	0.000	3085	1.07
6	PC	2.5E-04	1117.0	433.0	1550.0	1.892	0.494	0.653	0.273	0.720	0.000	0.000	26	29.00
13		6.7E-03	804.0	215.0	1019.0	0.824	0.581	0.218	0.072	0.166	0.000	0.000	123	3.70
10		4.6E-03	628.0	434.0	1062.0	0.736	0.617	0.114	0.043	0.036	0.000	0.000	502	30.40
18	CP	1.4E-04	499.0	1279.0	1778.0	2.240	1.029	1.212	0.192	0.000	1.020	0.000	9	17.75
20		7.0E-04	560.0	1161.0	1721.0	1.633	0.949	0.634	0.204	0.000	0.430	0.000	12	4.73
15		7.3E-04	337.0	1143.0	1440.0	1.760	0.340	1.140	0.212	0.000	0.928	0.000	20	7.50
23		1.4E-03	662.0	1205.0	1867.0	1.718	1.062	0.636	0.276	0.000	0.160	0.000	41	7.88
4		5.8E-03	553.0	1050.0	1603.0	1.299	0.928	0.371	0.091	0.000	0.280	0.000	259	12.30
22	CC	7.1E-04	670.0	693.0	1363.0	1.754	0.791	0.773	0.191	0.000	0.044	0.736	33	12.30
3		3.4E-03	609.0	623.0	1231.0	1.172	0.715	0.477	0.141	0.000	0.048	0.244	112	8.26
14		1.2E-02	521.0	521.0	1042.0	0.755	0.104	0.151	0.122	0.000	0.032	0.127	652	16.80
Cast IN 100, 925°C														
2	PP	5.0E-01	736.0	774.0	1510.0	2.170	0.924	1.246	1.246	0.000	0.000	0.000	15	3.21
32		5.0E-01	573.6	1192.0	1192.0	1.351	0.719	0.632	0.582	0.000	0.000	0.000	50	3.23
3		5.0E-01	493.0	520.0	1003.0	0.920	0.438	0.282	0.282	0.000	0.000	0.000	96	0.05
17		5.0E-01	548.7	569.1	1112.0	1.125	0.708	0.417	0.417	0.000	0.000	0.000	160	0.11
14		5.0E-01	395.3	403.7	789.0	0.640	0.500	0.140	0.140	0.000	0.000	0.000	300	0.17
36		5.0E-01	224.1	224.2	452.3	0.332	0.232	0.040	0.040	0.000	0.000	0.000	4015	2.23
24		5.0E-01	172.4	172.4	345.8	0.236	0.222	0.034	0.034	0.000	0.000	0.000	51261	28.36
74	PC	5.1E-04	504.7	241.3	746.0	1.324	0.481	0.643	0.207	0.436	0.000	0.000	22	12.02
13		4.4E-04	486.8	140.6	627.4	0.577	0.199	0.175	0.175	0.102	0.000	0.000	139	87.31
15		7.1E-04	412.3	141.3	553.6	0.450	0.152	0.394	0.394	0.064	0.000	0.000	332	129.11
93	CP	2.2E-04	322.7	474.3	947.0	2.100	0.643	1.657	0.169	0.000	1.288	0.600	6	6.09
11		1.0E-04	159.6	544.3	753.9	0.849	0.405	0.434	0.182	0.000	0.232	0.000	60	163.92
9		1.9E-03	142.0	360.6	502.6	0.414	0.320	0.094	0.094	0.000	0.047	0.000	1100	159.32
12	CC	1.4E-03	228.2	224.2	456.4	1.204	0.290	0.614	0.108	0.000	0.000	0.810	17	101.50
15		1.4E-04	171.0	171.0	342.0	0.650	0.218	0.432	0.218	0.019	0.000	0.374	102	203.37
43		1.0E-03	200.7	200.7	401.4	0.402	0.258	0.144	0.045	0.000	0.000	0.099	840	73.33
73	VERIF	2.8E-03	621.5	655.0	1276.5	1.625	0.423	0.602	0.577	0.107	0.000	0.018	17	1.73
72		2.8E-03	366.1	353.1	719.2	0.422	0.465	0.357	0.219	0.105	0.000	0.033	84	3.80
47		2.8E-03	345.4	251.2	596.6	0.517	0.190	0.127	0.059	0.043	0.000	0.030	454	47.11
75	VERIF	2.4E-03	415.4	532.6	1019.0	1.502	0.657	0.643	0.724	0.000	0.099	0.022	15	1.55
68		2.4E-03	375.1	452.6	817.7	0.860	0.540	0.326	0.191	0.000	0.132	0.013	74	7.97
56		2.4E-03	247.5	352.0	599.4	0.515	0.147	0.113	0.053	0.000	0.044	0.031	1400	140.00